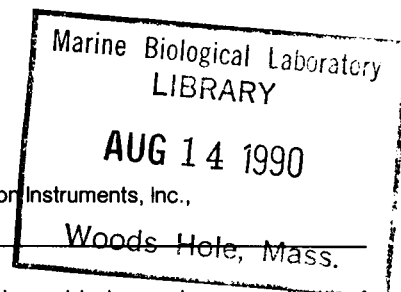


Optimizing planar lipid bilayer single-channel recordings for high resolution with rapid voltage steps

W. F. Wonderlin, A. Finkel,* and R. J. French

Department Medical Physiology, University of Calgary, Calgary, Alberta T2N 4N1 Canada; and *Axon Instruments, Inc., Foster City, California 94404 USA



ABSTRACT We describe two enhancements of the planar bilayer recording method which enable low-noise recordings of single-channel currents activated by voltage steps in planar bilayers formed on apertures in partitions separating two open chambers. First, we have refined a simple and effective procedure for making small bilayer apertures (25–80 μm diam) in plastic cups. These apertures combine the favorable properties of very thin edges, good mechanical strength, and low stray capacitance. In addition to enabling formation of small, low-capacitance bilayers, this aperture design also minimizes the access resistance to the bilayer, thereby improving the low-noise performance. Second, we have used a patch-clamp headstage modified to provide logic-controlled switching between a high-gain (50 G Ω) feedback resistor for high-resolution recording and a low-gain (50 M Ω) feedback resistor for rapid charging of the bilayer capacitance. The gain is switched from high to low before a voltage step and then back to high gain 25 μs after the step. With digital subtraction of the residual currents produced by the gain switching and electrostrictive changes in bilayer capacitance, we can achieve a steady current baseline within 1 ms after the voltage step. These enhancements broaden the range of experimental applications for the planar bilayer method by combining the high resolution previously attained only with small bilayers formed on pipette tips with the flexibility of experimental design possible with planar bilayers in open chambers. We illustrate application of these methods with recordings of the voltage-step activation of a voltage-gated potassium channel.

INTRODUCTION

The development, during the past 20 years, of methods which enable the recording of currents flowing through single ion channels has provided tools with which the processes underlying ion permeation and gating can be experimentally explored. The patch-clamp technique, in which a small patch of membrane containing one or more ion channels is isolated under the tip of a glass microelectrode, has been most widely used to obtain high-resolution, single-channel recordings. An alternate approach utilizes the incorporation of ion channels into an artificial, planar lipid bilayer, either by fusion of vesicles containing the channels with the membrane or by insertion of water-soluble channels. The planar bilayer method has played an important role in the field of ion channel physiology, predating the patch-clamp method for single-channel studies by several years (Bean et al., 1969). At present, some experimental requirements are better served by recording from single ion channels in planar bilayers than with the patch-clamp method (see Wonderlin et al., 1990, for further discussion). For example, using planar bilayers, the effect of membrane lipid properties (e.g., surface charge) on permeation and gating can be rigorously examined by varying the composition of the bilayer.

Also, single ion channels not directly accessible for patch clamping can be studied, either by fusion into planar bilayers of intact organelles (e.g., axonal transport vesicles, Wonderlin and French, 1989), or of vesicles prepared by membrane fractionation (e.g., skeletal muscle *t*-tubules or sarcoplasmic reticulum, reviewed in Miller, 1986). Finally, purified ion channels can be reconstituted into liposomes and fused into planar bilayers for study (e.g., Hartshorne et al., 1985).

The less widespread use of the planar bilayer method, compared to the patch method, results in part from its generally lower usable bandwidth and the difficulty in resolving single-channel currents activated by voltage steps. Both of these limitations result from the large electrical capacitance of planar bilayers, with diameters typically ranging from 80 to 300 μm (i.e., 40–560 pF at 0.8 $\mu\text{F}/\text{cm}^2$). One solution to this problem has been to form small (<20 μm diam) planar bilayers on the tips of patch pipettes, either by the "tip-dip" method, in which a pipette is twice passed through a lipid monolayer at an air/water interface (e.g., Coronado and Latorre, 1983) or by "punching" a pipette through a much larger, pre-formed bilayer (Mueller, 1975; Andersen, 1983; Green et al., 1987; Sigworth et al., 1987; Heinemann and Sigworth, 1988). These pipette-bilayer methods provide a significant reduction of background noise and shortening of the current settling time after a voltage-step, but they

Address correspondence to Dr. R. J. French, Dept. Medical Physiology, University of Calgary, Calgary, AB, T2N 4N1 Canada.

also introduce important experimental limitations compared to the method of forming bilayers over an aperture in a partition separating two open chambers. First, there is restricted access to the side of the bilayer bathed by the pipette solution. Second, the pipette bilayers may be too small to allow reasonable rates of direct channel incorporation by vesicle fusion. Rather, they require that channels be "captured" on a pipette tip while they reside in either a surface monolayer (which may denature some channels) or in a preformed bilayer. We report here two improvements which enhance both the signal resolution and our ability to examine voltage-step activation of ion channels in planar bilayers in open chambers. These improvements include a method for making small diameter bilayer apertures and a modified patch amplifier which allows rapid charging of the bilayer capacitance. With this method we can attain noise levels comparable to some pipette bilayer methods. Our method is demonstrated by an example of a high-resolution recording of the voltage-step activation of a K channel from squid nerve in a planar lipid bilayer.

METHOD FOR MAKING SMALL APERTURES WITH LOW STRAY CAPACITANCE IN RIGID PLASTIC PARTITIONS

In general, a planar bilayer is formed across an aperture in a plastic partition separating two solution-filled chambers. For the purpose of making small, low capacitance bilayers, an ideal design should have the following properties: (a) the margin of the aperture should be thin relative to the diameter of the aperture; (b) there should be a minimal amount of stray capacitance across the partition; and (c) the partition should have good mechanical strength. These are several reasons for favoring a thin margin of the aperture. First, because the bilayer forms within the aperture, a shortening of the aperture length decreases the distance from the bilayer surface to the well-stirred bulk solution in the chamber. This decreases the thickness of the poorly-stirred solution within the aperture, which can be a significant impediment to the diffusion of membrane vesicles from the bulk solution to the bilayer surface (Niles and Cohen, 1987). Second, a thin margin promotes bilayer thinning and the formation of a bilayer which occupies a relatively large fraction of the aperture area. Based on the modeling of annular shape presented by White (1972), the formation of a stable bilayer generally requires that the width of the annulus be less than one-half the length of the aperture. If, during bilayer formation, the width of the annulus is greater than this value, there will be an increased drainage of solvent from the annulus onto the partition, thereby

decreasing the volume and width of the annulus. Therefore, a thin aperture margin helps "drive" the formation of a bilayer occupying a large fraction of the aperture and having a small annular volume. Third, the settling time of the membrane current after a voltage step applied to a bilayer is often markedly increased by electrostrictive changes in bilayer capacitance which occur after the voltage step. This component of the transmembrane current generally exhibits a nonlinear dependence on applied voltage and may be difficult to subtract during analysis. According to White (1972), the application of a voltage across a bilayer increases the contact angle between the plane of the bilayer and the surface of the annulus, thereby narrowing the annulus and increasing the area of the bilayer and, hence, its capacitance. Because the magnitude of the electrostrictive change in membrane capacitance is proportional to the annular volume, a thin aperture margin and a relatively small annular volume reduces this effect. Finally, the electrical resistance of the aperture is proportional to its length and, as discussed below, the aperture resistance should be minimized.

Although apertures $>100\text{ }\mu\text{m}$ diam can be drilled or melted in plastic partitions, the requirement of a thin margin is not easily attained for smaller apertures, as the length of the aperture (i.e., thickness of the partition) may approach its diameter. This problem is not solved by simply using a thinner plastic partition, because of the increased stray capacitance across the thinner partition and, generally, an unsatisfactory reduction in mechanical strength. We have adapted and refined the method described by Neher et al. (1978), which enables the formation of very small apertures with very thin margins. Briefly, a conical metal stylus was warmed and pressed against the inner surface of a plastic cup, forming a cone-shaped depression extending partway across the cup wall (Fig. 1). The stylus was then removed and the plastic shaved from the outer surface until the depression

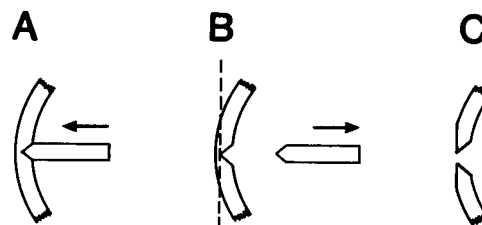


FIGURE 1 Aperture formation in a plastic cup (not drawn to scale). (A) A metal stylus is warmed and pressed against the inner surface of the cup, producing a cone-shaped depression. (B) After cooling, the stylus is retracted and the plastic shaved from the outer surface, leaving (C) a thin-edged aperture where the cut intersects the depression in the wall of the cup. See text for additional details.

was intersected. The size of the aperture was controlled by varying the depth of shaving. Additional details are described below. In addition to producing a small aperture with a thin margin, the rapidly increasing thickness of the plastic beyond the margin of the aperture decreased the stray capacitance across the partition (i.e., to <5 pF) and provided good mechanical strength.

The metal stylus should be constructed carefully, as its properties determine the quality of the aperture. High-quality styli were made from large (≈ 2 mm diam), stainless-steel darning needles. Compared to other types of steel, the hardness of the stainless steel made beveling more difficult, but improved the smoothness of the polished tip. To bevel the tip, the needle was placed in the chuck of a small electric drill held in a drill press (a small lathe could be substituted). The tip was then beveled using a series of grinding stones, finishing with a "Moon Stone" (W. R. Case and Sons Cutlery Co., Bradford PA). We found a tip angle of $\approx 80^\circ$ to be a good compromise between a shallow taper, which made controlling the size of the aperture easier, and a steeper taper, which increased the angle of opening of the cone-shaped depression. A tip diameter of ≈ 10 μm allowed apertures as small as ≈ 15 μm to be made. The finished stylus was cut to a length of 5 mm and soldered at a right angle to a steel shank, which was attached to a micromanipulator. This configuration aided positioning the stylus inside the cup. The shank was wrapped with 10 turns of magnet wire (26 gauge), and the stylus was heated by connecting the magnet wire to the current output of a microelectrode puller (David Kopf Instruments, Tujunga, CA).

With the plastic cup securely anchored with TackyWax on a platform, the stylus was warmed and pressed against the inner surface of the cup wall. The stylus was warmed only as much as required to allow the stylus to be slowly forced into the side of the cup. Excessive heating tended to degrade the plastic and produce a buildup of carbon on the stylus tip which can cause it to stick to the plastic. When the stylus had been pushed $\approx 3/4$ of the distance across the cup wall, the heat was turned off, and the stylus allowed to cool before it was removed from the cup. The cup was shaved with a disposable microtome blade (Feather, S35 Type, Fisher Scientific Co., Pittsburgh, PA) while being observed with a dissecting microscope. The distance to which the stylus is pushed into the wall can be varied. For cups with a larger radius, it may be more convenient to even push the stylus far enough to bulge the side of the cup outward, thereby decreasing the width of the plastic that will be in contact with the microtome blade. Further treatment of the aperture depended on the type of plastic used. We tested two types of plastic, polystyrene and high-density polyethylene (HDPE). We found that 12-mm polystyrene tubes (wall thickness, 0.75 mm), cut to a length of ≈ 1.5 cm, work

exceptionally well. Polystyrene's low melting temperature facilitated the melting of the depression, and its hardness produced a clean cut at the margin of the aperture. The apertures formed in polystyrene cups tended to have very sharp edges, 1–2 μm thick. These edges could be polished further by light heating (e.g., passing briefly by a hot air gun), but polishing did not appear to be necessary to form stable bilayers. Typically, crazing (i.e., appearance of small cracks) of the plastic at the margin of the aperture appeared with repeated use. Although moderate crazing did not decrease bilayer stability, the development of crazing could be reduced by warming the cup after aperture formation in a 60°C oven for 1 h. Small apertures were also formed in high-density polyethylene. HDPE tears slightly when cut with a knife, and these apertures needed to be heat polished to remove a ruffle of torn plastic at the edge of the aperture. Bilayers form very easily on HDPE, but were considerably less stable than bilayers on polystyrene. However, HDPE might be preferred in some situations because of its much greater solvent resistance. We have not tested other plastics with higher melting temperatures (e.g., Teflon).

Painted bilayers (lipids in decane) formed on small apertures in polystyrene cups were very stable, and provided single-channel recordings lasting from 2 to 4 h. A standard cleaning routine between experiments including cleaning the cups with detergent, and then rinsing sequentially with water; 1 N NaOH (optionally also stock 12 N HCl), distilled water, and ethanol. The chamber was then dried thoroughly under a stream of nitrogen. The formation of bilayers was facilitated by placing a small droplet (≈ 5 μl) of lipid dissolved in pentane (2 mg/ml) onto the dry aperture. After the pentane evaporated, the solutions were added to the chamber.

RECORDING SYSTEM

Electrical connections to the bath were made via miniature Ag/AgCl pellets (1 mm diam, In Vivo Metric, Healdsburg, CA) and salt bridges. Low-impedance bridges were constructed from disposable glass micropipettes (200 μl , ≈ 2 mm diam). One end of the pipette was sealed by fire polishing and cooled. Heat was then applied focally near the closed end, and air pressure was applied to the pipette until the thinned glass wall ruptured and a small hole (< 750 μm diam) was formed. The bridge was bent into an L shape, backfilled for ≈ 1.5 cm with 3 M KCl in 2% agar, and the remainder of the bridge was filled with 3 M KCl alone. The pellet was inserted to the end of the agar. A bridge constructed in this manner had a typical impedance of ≈ 200 Ω (100–10,000 Hz) in 3 M KCl.

For headstage amplifiers with a feedback resistor large enough to provide low-noise recordings (e.g., 10–50 G Ω),

the application of voltage steps across a large bilayer capacitance requires a large transient charging current that temporarily saturates the headstage amplifier and obscures rapidly-activating channel currents. With previous methods, even under good conditions, as much as 50 ms of single-channel activity may be lost after a voltage step due to a saturating current transient (e.g., Rosenberg et al., 1988). This charging time can be reduced by switching between high- and low-gain feedback resistors, depending on whether the immediate requirement is for low current noise or rapid charging of the membrane capacitance.

An Axopatch-1B amplifier with a CV-3B bilayer headstage (Axon Instruments, Inc., Burlingame, CA) was used. This is a commercially available headstage, constructed so that a logic pulse could trigger the rapid switching from a high-gain (50 G Ω) to a low-gain (50 M Ω) feedback resistor. The standard headstage was modified to enable an external TTL pulse to switch between the two feedback resistors. In the standard configuration, the resistors are switched by two field-effect transistors. One of these transistor switches is directly connected to the input and hence the bath solution. The control logic for these switches is normally slowed down so that the gate drive to the field-effect transistor that is connected to the bath takes several tens of milliseconds to change state. This minimizes the size of the switching current injected into the bath through the gate-to-source capacitance of the switch. In the modified version of the headstage, the switching time needed to be of the order of a few microseconds. At this faster rate, a significant current was injected into the input. This current was effectively canceled by connecting the inverse of the logic control signal to the input through a variable air capacitor. The capacitor was adjusted to minimize the switching transient observed at the output when the headstage was open circuited. The lower gain increased the maximum charging rate by 1,000 times, and the capacity current required for a 100-mV step across a 50-pF bilayer could be delivered in 25 μ s (assuming 10 V maximum headstage voltage). Consequently, the charging time after a step in command voltage was substantially reduced by overlapping the voltage step with a logic pulse which switched the feedback resistor to the lower gain just before the step and then switched back to the high gain after the charging current was nearly settled (15–70 μ s after the step for capacitances of 14–99 pF).

To evaluate the amplifier performance, we measured the duration of headstage saturation (without filtering) after a 100-mV voltage step across either a 14- or 99-pF ceramic capacitor using the CV-3B headstage. Without gain switching, the saturation durations were 3.9 and 49.7 ms, respectively. With gain switching, the sum of the charging time and the switching artifact was <200 μ s for

both capacitance values. Similarly rapid voltage changes should be attainable with recently available integrating headstages (i.e., using a capacitor to integrate the feedback current). For either the gain-switching resistive headstage or the integrating headstage, filtering can produce an undesirable increase in the apparent settling time because of the lag introduced by the rise time of the filter. This could be avoided by blanking the current transient before filtering.

Planar bilayers also exhibit electrostrictive changes in bilayer capacitance as a function of bilayer voltage. The electrostrictive changes in capacitance relax after a voltage step over a period of a few milliseconds to several seconds, depending on factors such as the size of the annulus. This component could be approximately removed by addition of currents produced by symmetric voltage steps or, preferably, because of its nonlinear voltage dependence, by subtraction of currents recorded when there was no channel activity.

MINIMIZING BACKGROUND CURRENT NOISE IN BILAYER RECORDINGS

Noise sources

The sources of background noise currents in the bilayer recording system can be divided into two groups. The first group includes the thermal noise currents in the headstage feedback resistor and bilayer resistance. These thermal noise currents are relatively insignificant because both resistances are large (>100 G Ω and 10–50 G Ω , respectively) and the spectral density of the thermal noise currents is flat. For example, if the bilayer resistance is 100 G Ω and the feedback resistance is 50 G Ω , the rms thermal noise current in these parallel resistances is only 0.05 pA in a 5-kHz bandwidth. The second group of noise current sources includes (a) the charging currents produced when the headstage input noise voltage is voltage clamped across the total input capacitance (C_i), and (b) the charging currents produced when the thermal voltage noise in the access resistance (R_a) is voltage clamped across the bilayer capacitance (C_m). These sources represent an important limitation of bilayer recording bandwidth because the bilayer capacitance is large and these sources have spectral densities that rise in proportion to the squares of both the bandwidth and the bilayer capacitance (Hamill et al., 1981; Levis, 1981; Sigworth, 1983; Rae and Levis, 1984).

The spectral density of the current noise produced by interaction of the headstage input voltage noise and the input capacitance is

$$S_{i(f)}^2 = e_n^2(2\pi C_i f)^2, \quad (1)$$

where C_i is the total input capacitance, f is the frequency, and e_n is the rms noise voltage ($V/\sqrt{\text{Hz}}$) in the headstage input. The input capacitance, C_i , is the sum of the FET input capacitance, the stray capacitance (e.g., across the partition), and the bilayer capacitance, C_m . The impedance term in this equation does not include the resistance, R_a , in series with C_m because, for typical values of R_a and C_m , the impedance of R_a in series with C_m is dominated by the reactive component.

The spectral density of the current noise produced by the thermal voltage noise of the access resistance in series with C_m is

$$S_{i(f)}^2 = 4kT \cdot \text{Re}\{Y(f)\}, \quad (2)$$

where $\text{Re}\{Y(f)\}$ is the real part of the admittance of R_a in series with C_m , and is given by

$$\text{Re}\{Y(f)\} = (\alpha^2) / [R_a(1 + \alpha^2)], \quad (3)$$

with $\alpha = 2\pi f R_a C_m$ (Hamill et al., 1981; Sigworth, 1983). For a constant bandwidth, at the lower limit of R_a (small α), $\text{Re}\{Y(f)\} = R_a(2\pi f C_m)^2$, and Eqs. 1 and 2 have a similar form. At the upper limit of R_a (large α), $\text{Re}\{Y(f)\} = 1/R_a$. The transition from a linear to a reciprocal dependence on R_a produces maxima in plots of this noise component against R_a (see Fig. 2A). For open bilayer chambers, the access resistance in series with the stray capacitance is very small (R_b , see below), hence we consider this source of noise to be dependent only on the bilayer capacitance, C_m .

The noise sources described in Eqs. 1 and 2 dominate the background noise of bilayer recordings and generally determine the usable bandwidth. The noise resulting from the headstage input voltage noise has been previously discussed in considerable detail, but the noise arising from the access resistance has not (but see Levis, 1981; Rae and Levis, 1984), especially in the context of the large

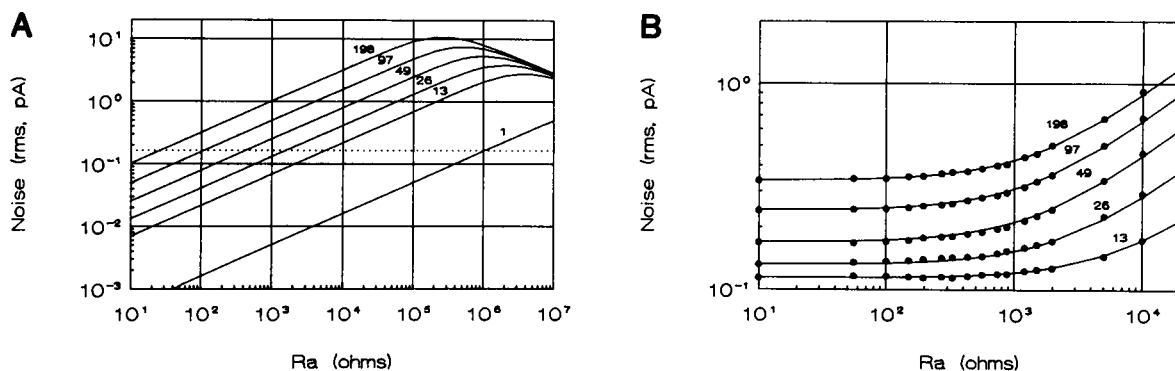


FIGURE 2 (A) The rms current noise (30 Hz–5 kHz bandwidth) arising only from interaction of the access resistance (R_a) and input capacitance (C_m) has been calculated, using Eq. 2, for several values of C_m (value shown above each curve) as a function of R_a (10 Ω –10 M Ω). The value of 1 pF has been included as an estimate of the combined capacitance of a relatively small pipette–bilayer and the pipette tip capacitance in series with the access resistance. The dotted line is drawn at the noise level produced by a 1 M Ω access resistance in series with the 1-pF capacitance. Note that this noise level is the same as that produced by a 13-pF bilayer ($\sim 40 \mu\text{m}$ diam) in series with a 6 k Ω access resistance (cf. resistance values in Table 1). (B) The total rms current noise (nominal 30 Hz–5 kHz bandwidth) in the output of the Axopatch amplifier produced by a series R_a – C_m input test circuit consisting of a ceramic capacitor and a carbon film resistor. These data (solid circles) were fit with curves which are the sum of (i) the rms noise with R_a equal to 10 Ω , which includes all other sources of background noise in the recording apparatus (e.g., noise in the feedback resistor, noise arising from headstage input noise voltage, and input capacitance), and (ii) the rms noise predicted by Eq. 2 and plotted in A. The measurements were made with the high-frequency boost adjusted to optimize the current step response produced by a triangle wave coupled to the input through a small capacitor (0.5 pF) in parallel with an input capacitance of 47 pF. The effective bandwidth used in this calculation takes into account the two-stage filtering produced by the bandwidth of the headstage, which decreases with increasing input capacitance, and the bandwidth of the rms meter input (30 Hz–5 kHz). The low-pass cutoff frequencies used for the integration of the noise density were estimated from the best fits and are listed below (similar values were obtained by an approximate calculation based on the overall rise time of the system).

C_m	Low-pass cutoff
pF	Hz
13	3550
26	3550
49	3200
97	2650
198	2000

capacitance of planar bilayers. In Fig. 2 *A* we have calculated the theoretical rms noise current (30 Hz–5 kHz), using Eq. 2, for several values of C_m as a function of R_a . The steep dependence of the magnitude of the rms noise current on both R_a and C_m is indicative of the importance of these factors in limiting the usable bandwidth of bilayer recordings. To determine if the extra noise observed experimentally in the presence of R_a could be accounted for by the relationship described in Eq. 2, we measured the rms noise in the output of the Axopatch amplifier as a function of access resistance and input capacitance, using a series R_a - C_m test circuit in which various values of ceramic capacitors and carbon film resistors were substituted. These data are shown in Fig. 2 *B*, with curves fitted as the sum of the background noise in the presence of a 10 Ω resistor and the noise predicted by Eq. 2. The close fit of these curves to the data confirm that the increased noise observed as a function of R_a can be accounted for by the relationship described in Eq. 2.

Both frequency-dependent noise sources can be reduced by decreasing the bilayer capacitance. However, because the capacitance is proportional to the square of the bilayer area, there is a diminishing reward for reducing the bilayer diameter much below ≈ 25 μm (i.e., ≈ 4 pF, assuming a specific capacitance of 0.8 $\mu\text{F}/\text{cm}^2$), as a result of the practical limitations of manipulating the bilayer (e.g., painting) and obtaining fusion of vesicles. Alternatively, the current noise can be reduced further by decreasing the noise voltage. With regard to the headstage input voltage noise, the degree to which this can be reduced is limited by the available semiconductor technology and the expense of state-of-the-art equipment, and control of this factor may be rather limited for the experimentalist. The access resistance, and its inherent thermal noise voltage, on the other hand, often can be reduced by careful consideration of the design of the bilayer recording system.

Minimizing access resistance

The access resistance is the sum of several resistances in series, including the electrode/electrolyte interface, the salt bridges, and the recording solution. Salt bridges (e.g., 3 M KCl) are essential for isolating the Ag/AgCl electrodes from the bath solutions and providing a constant, optimal environment for the electrode/electrolyte interface, minimizing both its impedance and the magnitude and drift of the junction potential. As described above, low-resistance (<200 Ω with 3 M KCl) salt bridges can be constructed. The resistance of the recording solution can be divided into three components based on geometrical considerations: (*a*) the resistance of the bulk bath solution (R_b) bathing each side of the partition; (*b*) the convergence resistance at each end of the aperture

(R_c); and (*c*) the resistance of the solution within the aperture (R_i).

We measured the resistance of several solutions commonly used in our experiments (Table 1). Only 10 mM Hepes, which is used to establish an osmotic gradient to promote vesicle/bilayer fusion, substantially increased R_b . For the other recording solutions, R_b makes only a small contribution to R_a . The most important contributors to the access resistance are the resistances associated with the bilayer aperture, R_c and R_i , as indicated by the substantial increase in the resistance with the addition of the partition and aperture (Table 1, column B). If the aperture is treated as a cylinder, the resistance within the aperture is $R_i = R_s(l/\pi a^2)$, where R_s is the specific resistance of the bath solution, and l and a are the length and radius of the aperture, respectively. The convergence resistance from the bulk solution to the plane of the mouth at either end of the aperture is given by $R_c = R_s/4a$ (Hall, 1975). The minimum aperture resistance, for a given diameter, is the sum of the two convergence resistances. For example, with $R_s = 30$ $\Omega\text{-cm}$ (symmetric solutions), values of $2R_c$ calculated for aperture diameters of 20, 40, and 80 μm diam are 15, 7.5, and 3.75 k Ω , respectively. Values of R_i , calculated for the same solution and aperture diameters, with an aperture length of 2 μm , are 1,910, 477, and 199 Ω . For this range of aperture dimensions, the dominant component of the access resistance is the convergence resistance. However, if the aperture is lengthened to 25 μm , which is the thickness of 1 mil Teflon tape, the access resistance for aperture

TABLE 1 Access resistance contributed by a 40- μm aperture

Solution	A. Bath only	B. With partition
	Ω	Ω
1 M NaCl	14.3	4.8×10^3
500 mM KAc	29.6	10.6×10^3
500 mM NaAc	42.9	14.4×10^3
200 mM NaCl	59.4	22.1×10^3
10 mM Na-Hepes (pH 7)	2.6×10^3	1.0×10^6

Resistance was measured as the real part of the impedance between two 1-mm-diam Ag/AgCl electrodes, using a model 4276A LCZ meter (Hewlett-Packard Co., Palo Alto, CA) with a 100-Hz test frequency. In column *A*, the resistance of 1 cm of each bath solution was calculated as the difference between the resistances measured when the electrodes were placed 5 and 15 mm apart in an open chamber. The difference calculation was used to remove the contribution of the resistance of the electrode/solution interface, which can be large relative to the resistance of the solutions alone. In column *B*, the resistance was measured between electrodes 1.2 cm apart in a recording chamber, using a cup with an aperture diameter of 40 μm . With addition of the partition, the access resistance increased by an average factor of ≈ 298 , which is 19% more than the increase expected for an optimal aperture resistance (i.e., $2R_c$, see text for discussion).

diameters below $\approx 20\ \mu\text{m}$ would be dominated by the intra-aperture resistance.

We examined the degree to which the resistance of a bilayer aperture ($40\ \mu\text{m}$ diam) formed by our method approaches the optimal value of $2R_c$ (Table 1). For all solutions, the addition of the partition and aperture increased the access resistance by an average of ≈ 298 times, which is only $\approx 19\%$ greater than the increase predicted by the sum of the convergence resistance alone. This discrepancy can be accounted for by the unilateral increase in convergence resistance produced by the angle of the opening formed by the stylus. The resistance of this mouth of the aperture is $R_c = R_s/(\pi\theta a)$, where θ is one-half the angle (in radians) of the opening (Purves, 1981). Other methods, such as drilling or melting a small hole in Teflon tape or forming bilayers on the tips of pipettes should produce higher resistances and higher current noise levels. For example, in symmetric 500 mM KAc, a $40\text{-}\mu\text{m}$ aperture formed by our method has a resistance of $10.6\ \text{k}\Omega$, whereas if it were formed as a $25\text{-}\mu\text{m}$ -long drilled hole or the tip of a glass pipette (6° tip angle), it would have an aperture resistance of 13 and $85\ \text{k}\Omega$, respectively. Thus, the characteristic shape of apertures formed by our shaving method results in access resistances more closely approaching the optimal (minimum) value for a given aperture diameter.

OTHER FACTORS AFFECTING BACKGROUND NOISE

In the course of refining our methods, we identified several potential sources of excess noise which could be eliminated. These are briefly discussed below.

Type of plastic. We initially observed that recordings in chambers made of acrylic (Lucite) were noisier than recordings in chambers made from HDPE. We subsequently performed a limited test of the excess noise properties of several types of plastics. A single well ($\approx 7\ \text{mm}$ diam) was drilled in each block of plastic and $0.5\ \text{ml}$ of $3\ \text{M}$ KCl was added to the well. The headstage input of an Axopatch 1-B amplifier was connected by a Ag-AgCl pellet to the solution in the well. The headstage and plastic block were positioned to minimize stray capacitance between the solution in the well and ground. Comparison of the rms noise ($30\ \text{Hz}$ – $5\ \text{kHz}$ bandwidth) among the various plastics revealed the following series, in order of increasing rms noise (relative to HDPE): polystyrene (1.0) = polycarbonate (1.0) = Teflon (1.0) < acrylic (1.4) < nylon (1.5).

Solvent. Although the rms noise is usually proportional to membrane capacitance, we have often observed a decrease in noise as the membrane capacitance increased during the late stages of bilayer thinning. Apparently,

there is a component of the background current noise whose magnitude is inversely dependent on the specific capacitance of the bilayer. The noise level can sometimes be reduced by rewiping a bilayer painted from lipids in decane with a small amount of a higher molecular-weight solvent, such as hexadecane or squalene, which partitions to a lesser extent into the bilayer. This usually produces a bilayer with a higher specific and total capacitance, but, paradoxically, with a lower noise.

Vibration. Smaller bilayers are generally less sensitive to vibration. However, an easily overlooked source of vibrational noise is the meniscus at the junction of the solution surface and the chamber wall. In the case of strongly hydrophobic plastics (e.g., polystyrene), the contact angle between the solution surface and the cup wall is large (i.e., near 90°). Under this condition, the meniscus may appear uneven or "strained." Vibrational stimulation causes the height of the strained meniscus to fluctuate in discrete, irregular jumps, and these rapid movements are very effective in producing a vibrational artifact. This artifact can be reduced by adding a small amount ($\approx 5\ \mu\text{l}$) of dilute lipid ($2\ \text{mg/ml}$) in pentane to the surface (Fig. 3). The lipid monolayer which forms after evaporation of the pentane decreases the contact angle between the solution surface and the cup wall, presumably by reducing the surface tension. With the smoother meniscus, both the irregular fluctuations in meniscus height and the sensitivity to vibrational noise are markedly reduced. It is likely that any method for making the cup wall wettable by the bath solution would also be

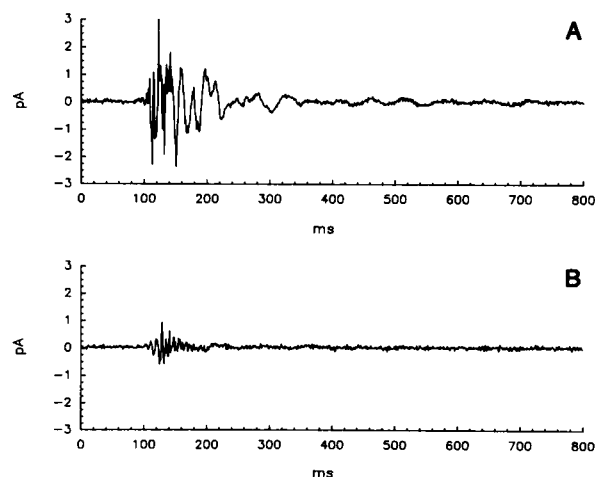


FIGURE 3 Sensitivity of bilayer recording to vibrational stimulation. (A) Vibrational artifact produced by dropping a book (Sakmann and Neher, 1983) from a height of $10\ \text{cm}$ onto the table surface next to the bilayer recording apparatus. (B) The amplitude of the vibrational artifact from an identical stimulus is reduced after formation of a phospholipid monolayer on the surface of both bath solutions.

effective, as the sensitivity to vibration can also be reduced by making the wall of the cup hydrophilic in the absence of a surface lipid monolayer (data not shown).

VOLTAGE STEP ACTIVATION OF ION CHANNELS FROM SQUID AXOPLASM

Axoplasmic organelles were prepared from giant axons of *Loligo pealei* as previously described (Wonderlin and French, 1989). Briefly, axoplasm was extruded using the roller method, and the cytoskeleton was depolymerized by gentle trituration in a K-iodide buffer. Dense material was removed by low-speed centrifugation (5' at 1,300 *g*). Incorporation was achieved by squirting small amounts (1–3 μ l) of the supernatant from a pipette held close to the bilayer. Planar lipid bilayers were formed by painting a solution of synthetic lipids, phosphatidylethanolamine:phosphatidylcholine (PE:PC, 80:20), in decane (50 mg/ml) over an aperture pretreated with the same lipids in a dilute pentane solution (2 mg/ml).

The activation of a voltage-dependent K channel is shown in Fig. 4. The input capacitance (bilayer and stray sources) is ≈ 35 pF and the rms noise is 0.37 pA (noise measured for an effective system bandwidth of ~ 30 –3,400 Hz). For comparison, a recent implementation of the bilayer punch method for studies on incorporated channels yields rms noise levels of ~ 0.6 pA in a bandwidth of 0–5,000 Hz (Andersen, O. S., personal communication). The records shown in Fig. 4 have been filtered at 2.5 kHz with an eight-pole Bessel filter and sampled at 40 kHz. In Fig. 4 *A*, the current response to a step from -100 to -65 mV is shown without digital subtraction. The headstage was switched to low gain 1 ms before the voltage step, producing a small, spikelike switching artifact preceding the larger capacity transient produced by the voltage step. The headstage was switched back to high gain 25 μ s after the voltage step. In Fig. 4 *B*, most of the remaining transient has been removed by subtraction of the average of blank (no channel activation) records. We have found that for bilayer capacitances < 50 pF, we can routinely achieve a steady current level within 1 ms after the voltage step. In Fig. 4 *C*, 240 records have been subtracted and averaged to mimic the time course of a "macroscopic" K current.

CONCLUSIONS

We have shown that low-noise recordings with voltage-step activation of ion channels can be achieved using planar lipid bilayers in an open chamber design. We have reduced the background noise to a level within the range

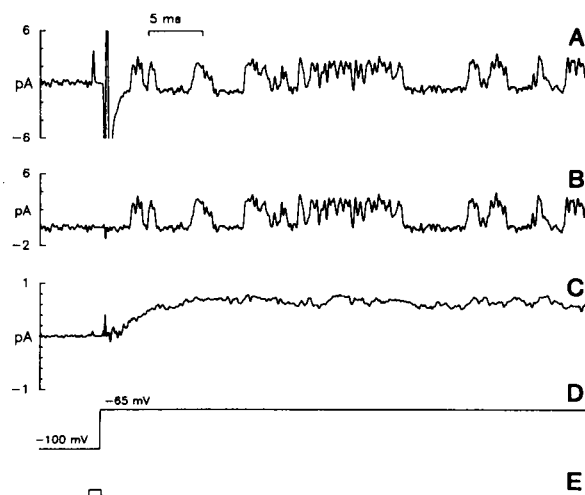


FIGURE 4 Voltage-step activation of a K channel from squid giant axon axoplasm. (*A*) A single, unsubtracted current record showing the response to a voltage step. In *A*–*C*, the current is actually inward, but is shown inverted to be consistent with the usual orientation of K current records. The gain was switched to low 1 ms before the voltage step, producing a small current transient (logic pulse is shown in trace *E*). The gain was switched back to high 25 μ s after the voltage step. (*B*) Current record from which the capacitive current and switching artifact have been digitally subtracted. Blank traces (seven traces in which the channel was not active) were averaged and subtracted from the active trace. Subtraction is very effective in removing the step artifact, and high-resolution recording is established within 1 ms after the voltage step. (*C*) An average current record simulating a macroscopic response. 240 current tracks were averaged, from which the average of the blank records was subtracted, as in *B*. (*D*) Voltage command trace. (*E*) Logic pulse used to switch the headstage gain. The headstage was switched to low gain during the rectangular pulse.

reported for several pipette-bilayer applications, while using bilayers with a diameter (40–80 μ m) large enough to permit relatively easy fusion of vesicles and incorporation of ion channels. To attain optimal low-noise performance with these small bilayers requires minimization of the current noise generated by the voltage noise in the access resistance in series with the bilayer capacitance, which accounts for at least one-half the background current noise under many bilayer recording conditions. Similarly, low levels of noise from this source can be attained either with an open chamber design, in which the bilayer capacitance is reduced to a relatively small value (10–40 pF) and the access resistance is minimized (5–20 k Ω), or with the pipette-bilayer methods, where the bilayer capacitance is greatly reduced (0.1–6 pF) at the expense of a large increase in the access resistance within the pipette (200 k Ω –5 M Ω). The small bilayers we have used appreciably decrease the settling time after a voltage step. However, a much more significant reduction in settling time was attained by using a headstage with

logic-controlled switching between high-gain (50 G Ω) and low-gain (50 M Ω) feedback resistors, which increases the rate of charging of the bilayer capacitance by 1,000-fold.

We thank Dr. Christopher Miller for prompting us to think about the role of the access resistance in generating noise across bilayers. We also thank Dr. R. Clark and Dr. L. Haynes for reading a draft of the manuscript. Mr. Richard Lobdill's assistance in the engineering implementation of the headstage modification was appreciated.

This research was supported by an operating grant from the Medical Research Council of Canada (grant MA-10053) and an Implementation Grant from the Alberta Heritage Foundation for Medical Research (AHFMR). W. F. Wonderlin is an AHFMR Fellow and R. J. French is an AHFMR Scholar.

Received for publication 18 December 1989 and in final form 11 April 1990.

REFERENCES

- Andersen, O. S. 1983. Ion movement through gramicidin A channels. Single-channel measurements at very high potentials. *Biophys. J.* 41:119-133.
- Bean, R. C., W. C. Shepherd, H. Chan, and J. Eichner. 1969. Discrete conductance fluctuations in lipid bilayer protein membranes. *J. Gen. Physiol.* 53:741-757.
- Coronado, R., and R. Latorre. 1983. Phospholipid bilayers made from monolayers on patch-clamp pipettes. *Biophys. J.* 43:231-236.
- Green, W. N., L. B. Weiss, and O. S. Andersen. 1987. Batrachotoxin-modified sodium channels in planar lipid bilayers. Ion permeation and block. *J. Gen. Physiol.* 89:841-872.
- Hall, J. E. 1975. Access resistance of a small circular pore. *J. Gen. Physiol.* 66:531-532.
- Hamill, O. P., A. Marty, E. Neher, B. Sakmann, and R. J. Sigworth. 1981. Improved patch-clamp techniques for high-resolution current recording from cells and cell-free membrane patches. *Pfluegers Arch. Eur. J. Physiol.* 391:85-100.
- Hartshorne, R. P., B. U. Keller, J. A. Talvenheimo, W. A. Catterall, and M. Montal. 1985. Functional reconstitution of the purified brain sodium channel in planar lipid bilayers. *Proc. Natl. Acad. Sci. USA.* 82:240-244.
- Heinemann, S. H., and F. J. Sigworth. 1988. Estimation of Na⁺ dwell time in the gramicidin A channel. Na⁺ ions as blockers of H⁺ currents. *Biochim. Biophys. Acta.* 987:8-14.
- Levis, R. A. 1981. Patch and axial wire voltage clamp techniques and impedance measurements of cardiac purkinje fibers. Part III. Dynamic and noise performance of a patch voltage clamp. Ph.D. thesis, University of California, Los Angeles. University Microfilms International, Ann Arbor, MI.
- Miller, C. 1986. Ion Channel Reconstitution. Plenum Publishing Corp., New York. 577 pp.
- Mueller, P. 1975. Membrane excitation through voltage-induced aggregation of channel precursors. *Ann. NY Acad. Sci.* 264:246-264.
- Neher, E., J. Sandblom, and G. Eisenman. 1978. Ionic selectivity, saturation, and block in gramicidin A channels. II. Saturation behavior of single channel conductances and evidence for the existence of multiple binding sites in the channel. *J. Membr. Biol.* 40:97-116.
- Niles, W. D., and F. S. Cohen. 1987. Video fluorescence microscopy studies of phospholipid vesicle fusion with a planar phospholipid membrane. *J. Gen. Physiol.* 90:703-735.
- Purves, R. D. 1981. Microelectrode Methods for Intracellular Recording and Ionophoresis. Academic Press, Inc., London. 146 pp.
- Rae, J. L., and R. A. Levis. 1984. Patch voltage clamp of lens epithelial cells: theory and practice. *Mol. Physiol.* 6:115-162.
- Rosenberg, R. L., P. Hess, and R. W. Tsien. 1988. Cardiac calcium channels in planar lipid bilayers. L-Type channels and calcium-permeable channels open at negative membrane potentials. *J. Gen. Physiol.* 92:27-54.
- Sakmann, B., and E. Neher. 1983. Single-Channel Recording. Plenum Publishing Corp., New York. 503 pp.
- Sigworth, F. J. 1983. Electronic design of the patch clamp. In *Single-Channel Recording*. B. Sakmann and E. Neher, editors. Plenum Publishing Corp., New York. 3-35.
- Sigworth, F. J., D. W. Urry, and K. U. Prasad. 1987. Open channel noise. III. High resolution recordings show rapid current fluctuations in gramicidin A and four chemical analogues. *Biophys. J.* 52:1055-1064.
- White, S. H. 1972. Analysis of the torus surrounding planar lipid bilayer membranes. *Biophys. J.* 12:432-445.
- Wonderlin, W. F., and R. J. French. 1989. Voltage-gated Na⁺ and K⁺ channels from the axoplasm of *Loligo pealei*. *Biophys. J.* 55:317a. (Abstr.)
- Wonderlin, W. F., R. J. French, and N. J. Arispe. 1990. Recording and analysis of currents from single ion channels. *Neuromethods*. In press.